

Modeling the effects of parathyroid hormone and calcitonin on calcium homeostasis

Inthira Chaiya, Chontita Rattanakul, Sahattaya Rattanamongkonkul, Wannapa Panitsupakamon,

and Sittipong Ruktamatakul

Abstract—In this paper, we propose a system of ordinary differential equations in order to describe calcium homeostasis by considering parathyroid hormone and calcitonin as two major regulating hormones. Geometric singular perturbation is utilized in order to obtain the conditions on the system parameters that differentiate various kinds of dynamic behavior. Numerical simulations are also carried out to confirm our theoretical predictions.

Keywords—Calcitonin, calcium homeostasis, mathematical model, parathyroid hormone.

I. INTRODUCTION

MAINTAINING the normal level of calcium ion in extracellular fluid is essential for human. Calcium in its ionized form plays very important role in regulating of enzymatic activities and fundamental cellular events such as muscular contraction, secretion and cell division [1]-[4]. Too high or too low of serum levels of calcium indicate hypercalcemia or hypocalcemia, respectively [1]-[4]. Hence, the understanding of calcium homeostasis, the process that controls the normal level of serum calcium, is needed.

Many factors involve in calcium homeostasis including parathyroid hormone (PTH), calcitonin (CT) [1]-[5]. To maintain the serum level of calcium in the normal range, PTH

This work was supported by the Centre of Excellence in Mathematics, Commission on Higher Education, Thailand and the Royal Golden Jubilee Ph.D. Program (contract number PHD53K0191).

I. Chaiya is with the Department of Mathematics, Faculty of Science, Mahidol University, Thailand and the Centre of Excellence in Mathematics, the Commission on Higher Education, Thailand (e-mail: g5438789@student.mahidol.ac.th).

C. Rattanakul is with the Department of Mathematics, Faculty of Science, Mahidol University, Thailand and the Centre of Excellence in Mathematics, the Commission on Higher Education, Thailand (corresponding author, phone: 662-201-5340; fax: 662-201-5343; e-mail: chontita.rat@mahidol.ac.th).

S. Rattanamongkonkul is with the Department of Mathematics, Faculty of Science, Burapha University, Thailand and the Centre of Excellence in Mathematics, the Commission on Higher Education, Thailand (e-mail: sahattay@buu.ac.th).

W. Panitsupakamon is with the Department of Mathematics, Faculty of Science, Silpakorn University, Thailand and the Centre of Excellence in Mathematics, the Commission on Higher Education, Thailand (e-mail: wannapa@su.ac.th).

S. Ruktamatakul is with the Department of Mathematics, Faculty of Liberal Arts Science, Kasetsart University, Thailand and the Centre of Excellence in Mathematics, the Commission on Higher Education, Thailand (e-mail: faasspr@nontri.ku.ac.th).

acts directly on bone to stimulate bone resorption activity. It also acts directly on kidney to stimulate the reabsorption of calcium from urine and acts indirectly on intestine to enhance the conversion of vitamin D into its active form resulting in the increase of calcium absorption from diet [1]-[5]. CT, on the other hand, acts directly on bone to inhibit bone resorption activity. In this paper, a mathematical model is then developed in order to get the better understanding of calcium homeostasis based upon the effects of two hormones, PTH and CT.

II. MODEL DEVELOPMENT

Calcium homeostasis is the process that keeps the serum level of calcium in the normal range. The factors that will be taken in to account here are PTH and CT.

When the serum level of calcium falls below the normal range, PTH is then released from the parathyroid glands and binds with its receptors at the target organs which are bone, kidney and intestine [1]-[5]. The serum level of calcium is then raised to the normal level. On the other hand, when the serum level of calcium raises above the normal range, CT is then secreted from the parafollicular cells of the thyroid gland and inhibits bone resorption activity. The serum level of calcium is then decreased to the normal range [1]-[5].

Let us denote the concentration of PTH above the basal level in blood at time t by $X(t)$, the concentration of CT in blood at time t by $Y(t)$ and the concentration of calcium ion in blood at time t by $Z(t)$. The following system of nonlinear ordinary differential equations is then use to investigate calcium homeostasis based upon the effects of parathyroid hormone and calcitonin:

$$\frac{dX}{dt} = \frac{a_1}{k_1 + Z} - b_1 X \quad (1)$$

$$\frac{dY}{dt} = (a_2 - a_3 Y) Y Z - b_2 Y \quad (2)$$

$$\frac{dZ}{dt} = \left(\frac{a_4 + a_5 X}{k_2 + X^2} - a_6 Y \right) Z - b_3 Z \quad (3)$$

Note that all parameters in the system are assumed to be positive.

The rate of change of the serum level of PTH above the basal level at time t is described by (1). On the right hand side, the first term represents the secretion rate of PTH from the

parathyroid glands in response to the serum level of calcium. When the serum calcium level is high the secretion rate of PTH will be decreased in order to counter balance the high level of calcium in blood. The last term represents the removal rate of PTH from the system.

The rate of change of the serum level of CT at time t is described by (2). On the right hand side, the first term represents the secretion rate of CT in response to the level of calcium. When the serum level is high, the secretion of CT will be increased in order to counter balance the high level of calcium in blood. The last term represents the removal rate of CT from the system.

The rate of change of the serum level of calcium at time t is described by (3). On the right hand side, the first term represents the rate of change in calcium level due to the effects of PTH and CT. The last term represents the removal rate of calcium from the system.

III. ANALYSIS OF THE MODEL

Assuming that the dynamic of PTH is fast, the dynamic of CT is intermediate and the dynamic of calcium is slow. We then scale the dynamics of the three components and parameters of the system (1)-(3) in term of small positive parameters $0 < \varepsilon \ll 1$ and $0 < \delta \ll 1$ as follows.

Letting $x = X$, $y = Y$, $z = Z$, $c_1 = a_1$, $c_2 = \frac{a_2}{\varepsilon}$, $c_3 = \frac{a_3}{\varepsilon}$,

$c_4 = \frac{a_4}{\varepsilon\delta}$, $c_5 = \frac{a_5}{\varepsilon\delta}$, $c_6 = \frac{a_6}{\varepsilon\delta}$, $d_1 = b_1$, $d_2 = \frac{b_2}{\varepsilon}$, $d_3 = \frac{b_3}{\varepsilon\delta}$, the system (1)-(3) becomes

$$\frac{dx}{dt} = \frac{c_1}{k_1 + z} - d_1 x \equiv F(x, y, z) \quad (4)$$

$$\frac{dy}{dt} = \varepsilon((c_2 - c_3 y)yz - d_2 y) \equiv \varepsilon G(x, y, z) \quad (5)$$

$$\frac{dz}{dt} = \varepsilon\delta\left(\left(\frac{c_4 + c_5 x}{k_2 + x^2} - c_6 y\right)z - d_3 z\right) \equiv \varepsilon\delta H(x, y, z) \quad (6)$$

The system (4)-(6) can then be analyzed by using the geometric singular perturbation method [6], [7].

Note that the shapes, directions and speeds of the solution trajectories of the system are determined by the shapes and the relative position of the manifold $\{F=0\}$, $\{G=0\}$, and $\{H=0\}$. Therefore, we shall investigate each manifold in detail.

The manifold $\{F=0\}$

This manifold is given by the equation

$$x = \frac{c_1}{d_1(k_1 + z)} \equiv A_1(z) \quad (7)$$

We can see that this manifold is independent of the variable y and hence it is parallel to the y -axis. In addition, it intersects the x -axis at the point where

$$x = \frac{c_1}{d_1 k_1} \equiv x_1 \quad (8)$$

Note that $A_1(z)$ is an decreasing function of z and $A_1(z) \rightarrow 0$ as $z \rightarrow \infty$.

The manifold $\{G=0\}$

This manifold consists of two sub-manifolds. One is the trivial manifold $y=0$. The other one is the nontrivial manifold given by the equation

$$z = \frac{d_2}{c_2 - c_3 y} \equiv A_2(y) \quad (9)$$

We can see that the nontrivial manifold is independent of the variable x and hence, it is parallel to the x -axis. In addition, its intersects the z -axis at the point where

$$z = \frac{d_2}{c_2} \equiv z_1 \quad (10)$$

Note that $A_2(y)$ is an decreasing function of y and

$A_2(y) \rightarrow \infty$ as $y \rightarrow y_1^-$ where $y_1 = \frac{c_2}{c_3}$.

Moreover, the manifold $\{F=0\}$ intersects the manifold $\{G=0\}$ along the curve

$$\left\{ x = \frac{c_1}{d_1(k_1 + z)}, y = 0 \right\} \quad (11)$$

and the curve,

$$\left\{ x = \frac{c_1}{d_1(k_1 + z)}, z = \frac{d_2}{c_2 - c_3 y} \right\} \quad (12)$$

The manifold $\{H=0\}$

This manifold consists of two sub-manifolds. One is the trivial manifold $z=0$. The other one is the nontrivial manifold

$$y = \frac{1}{c_6} \left(\frac{c_4 + c_5 x}{k_2 + x^2} - d_3 \right) \equiv A_3(x) \quad (13)$$

We can see that the nontrivial manifold is independent of the variable z and hence it is parallel to the z -axis. $A_3(x)$ attains its relative maximum at the points where

$$x = \frac{-c_4 + \sqrt{c_4^2 + c_5^2 k_2}}{c_5} \equiv x_M \quad (14)$$

and

$$y = \frac{1}{c_6} \left(\frac{c_4 + c_5 x_M}{k_2 + x_M^2} - d_3 \right) \equiv y_M \quad (15)$$

Note that $y_M > 0$ if and only if

$$c_4 > d_3(k_2 + x_M^2) - c_5 x_M \quad (16)$$

Moreover, the nontrivial manifold $y = A_3(x)$ intersects the y -axis at the point where

$$y = \frac{1}{c_6} \left(\frac{c_4}{k_2} - d_3 \right) \equiv y_2 \quad (17)$$

Note that $y_2 > 0$ if and only if

$$c_4 > d_3 k_2 \quad (18)$$

In addition, the nontrivial manifold $y = A_3(x)$ intersects the $x -$ axis at the point where

$$x = \frac{c_5 + \sqrt{c_5^2 + 4d_3(c_4 - d_3k_2)}}{2d_3} \equiv x_2 \tag{19}$$

Note that if $y_2 > 0$ then $x_2 > 0$.

The manifold $\{F = 0\}$ intersects the manifold $\{H = 0\}$ along the line

$$\{x = x_1, z = 0\}$$

and the curve

$$\left\{ x = \frac{c_1}{d_1(k_1 + z)}, y = \frac{1}{c_6} \left[\left(\frac{c_4 + c_5x}{k_2 + x^2} \right) - d_3 \right] \right\}$$

which attains its relative maximum at the points where $x = x_M, y = y_M$, and

$$z = \frac{1}{d_1} \left(\frac{c_1}{x_M} - d_1k_1 \right) \equiv z_M \tag{20}$$

Note that $z_M > 0$ if and only if

$$x_M < x_1 \tag{21}$$

On the other hand, the manifold $\{F = 0\}$ intersects the manifold $\{G = 0\}$ and the manifold $\{H = 0\}$ at the points $(x_1, 0, 0), (x_2, 0, z_{s_1})$ and $(x_{s_2}, y_{s_2}, z_{s_2})$ where

$$z_{s_1} = \frac{c_1}{d_1x_2} - k_1 \tag{22}$$

x_{s_2} is a positive solution of

$$Ax^3 + Bx^2 + Cx + D = 0 \tag{23}$$

where

$$A = -(c_6d_1d_2 + c_3d_1d_3k_1 - c_2d_1k_1) < 0$$

$$B = c_1c_2 + c_3c_5d_1k_1 + c_1c_3d_3 > 0$$

$$C = c_3c_4d_1k_1 - (c_2d_1k_1k_2 + c_6d_1d_2k_2 + c_1c_3c_5 + c_3d_1d_3k_1k_2)$$

$$D = c_1c_2k_2 + c_1c_3d_3k_2 - c_1c_3c_4$$

and $y_{s_2} = \frac{1}{c_6} \left(\frac{c_4 + c_5x_{s_2}}{k_2 + x_{s_2}^2} - d_3 \right), z_{s_2} = \frac{c_1}{d_1x_{s_2}} - k_1.$

Note that x_{s_2} exists in the first octant provided that

$$D > 0 \tag{24}$$

and $y_{s_2} > 0$ if

$$c_4 + c_5x_{s_2} > d_3(k_2 + x_{s_2}^2) \tag{25}$$

and $z_{s_2} > 0$ if

$$x_{s_2} < x_1 \tag{26}$$

Case 1 If ε and δ are sufficiently small, and

$$x_M < x_1 < x_2 \tag{27}$$

$$z_{s_2} < z_M \tag{28}$$

provided that the inequalities (16), (18) and (24)-(26) are satisfied where all parametric values are defined as above, then a periodic solution exists for the system of (4)-(6).

If all inequalities identified in Case 1 hold, then the manifolds $\{F = 0\}, \{G = 0\}$ and $\{H = 0\}$ are positioned as in Fig. 1. Starting from the point A in front of the manifold $\{F = 0\}$. Since $\{F < 0\}$ here, a fast transition will bring the system to the point B on the manifold $\{F = 0\}$ in the direction of decreasing x . Here, $\{G < 0\}$ and a transition at intermediate speed will be made in the direction of decreasing y until point C on the curve $\{F = H = 0\}$ is reached. An intermediate transition then follows along this curve to some point D on the other stable part of $\{F = H = 0\}$ followed by an intermediate transition in the direction of decreasing y until the point E is reached since $\{G < 0\}$ here. Once the point E is reached the stability of sub-manifold will be lost. A jump to point F on the other stable part of $\{F = H = 0\}$ followed by an intermediate transition in the direction of increasing y since $\{G > 0\}$ here. Once the point G is reached the stability of sub-manifold will be lost. A jump to point H on the other stable part of $\{F = H = 0\}$. Consequently, an intermediate transition will bring the system back to the point E , followed by flows along the same path repeatedly, resulting in the closed orbit $EFGHE$. Thus, limit cycle in the system for ε and δ are sufficiently small exists.

Case 2 If ε and δ are sufficiently small, and

$$x_M < x_1 < x_2 \tag{29}$$

$$z_M < z_{s_2} \tag{30}$$

provided that the inequalities (16), (18) and (24)-(26) are satisfied where all parametric values are defined as above, then a stable equilibrium point exists for the system of (4)-(6).

If all inequalities identified in Case 2 hold, then the manifolds $\{F = 0\}, \{G = 0\}$ and $\{H = 0\}$ are positioned as in Fig. 2. Starting from point A in front of the manifold $\{F = 0\}$. Since $\{F < 0\}$ here, a fast transition will bring the system to the point B on the manifold $\{F = 0\}$ in the direction of decreasing x . Here, $\{G < 0\}$ and a transition at intermediate speed will be made in the direction of decreasing y until point C on the curve $\{F = H = 0\}$ is reached. An intermediate transition then follows along this curve to some point D on the other stable part of $\{F = H = 0\}$ followed by an intermediate transition in the direction of decreasing y until the point E is reached since $\{G < 0\}$ here. Once the point E is reached the stability of sub-manifold will be lost. A jump to point F on the other stable part of $\{F = H = 0\}$ followed by an intermediate transition in the direction of increasing y until the steady state S_2 where $\{F = G = H = 0\}$ is reached since $\{G > 0\}$ here. Thus, the solution trajectory is expected in this case to tend toward this stable equilibrium point S_2 as time passes.

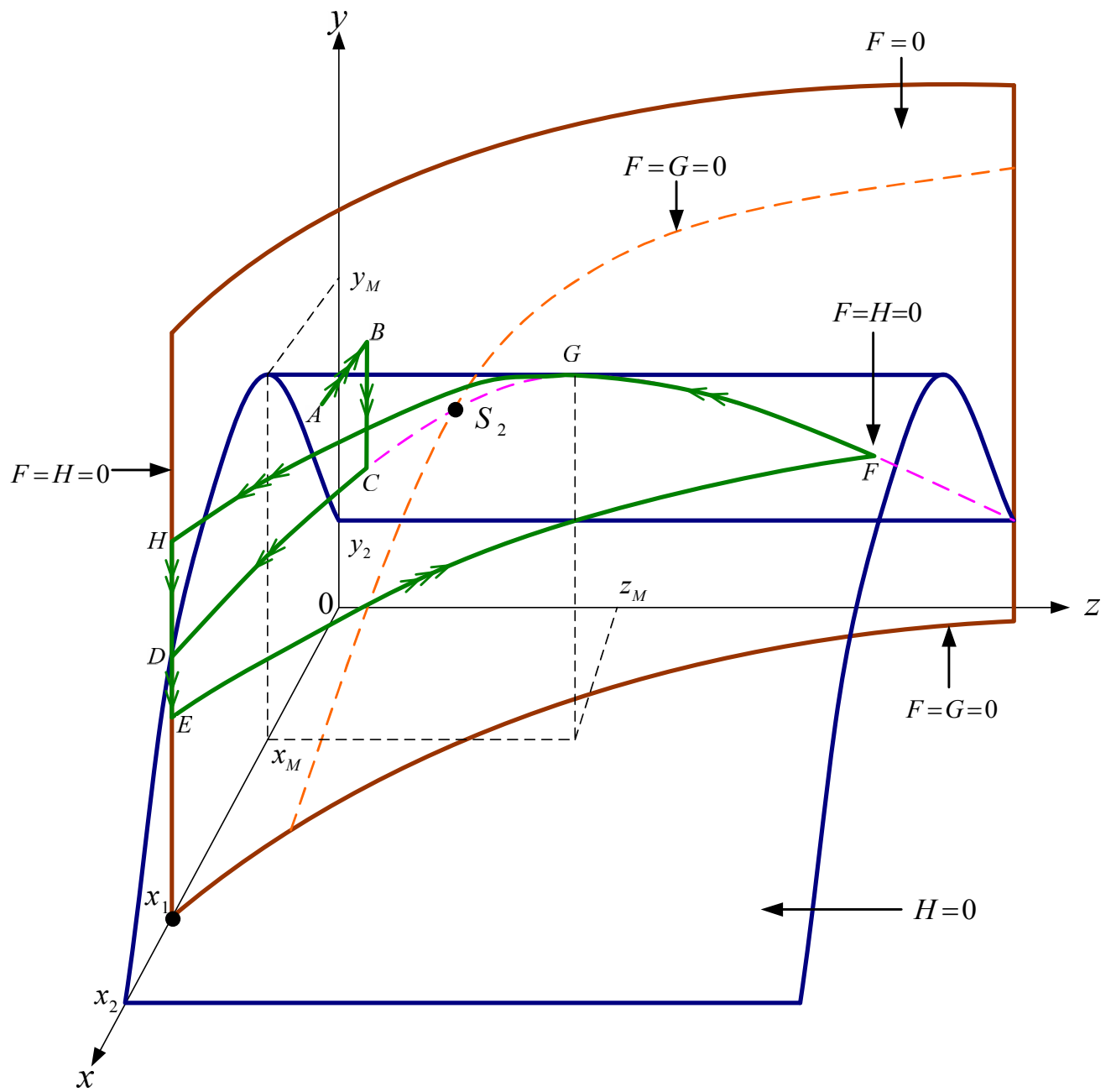


Fig. 1 The three equilibrium manifolds $\{F=0\}, \{G=0\}$ and $\{H=0\}$ in (x, y, z) -space in Case 1. Segments of the trajectories with one, two, and three arrows represent slow, intermediate, and fast transitions, respectively.

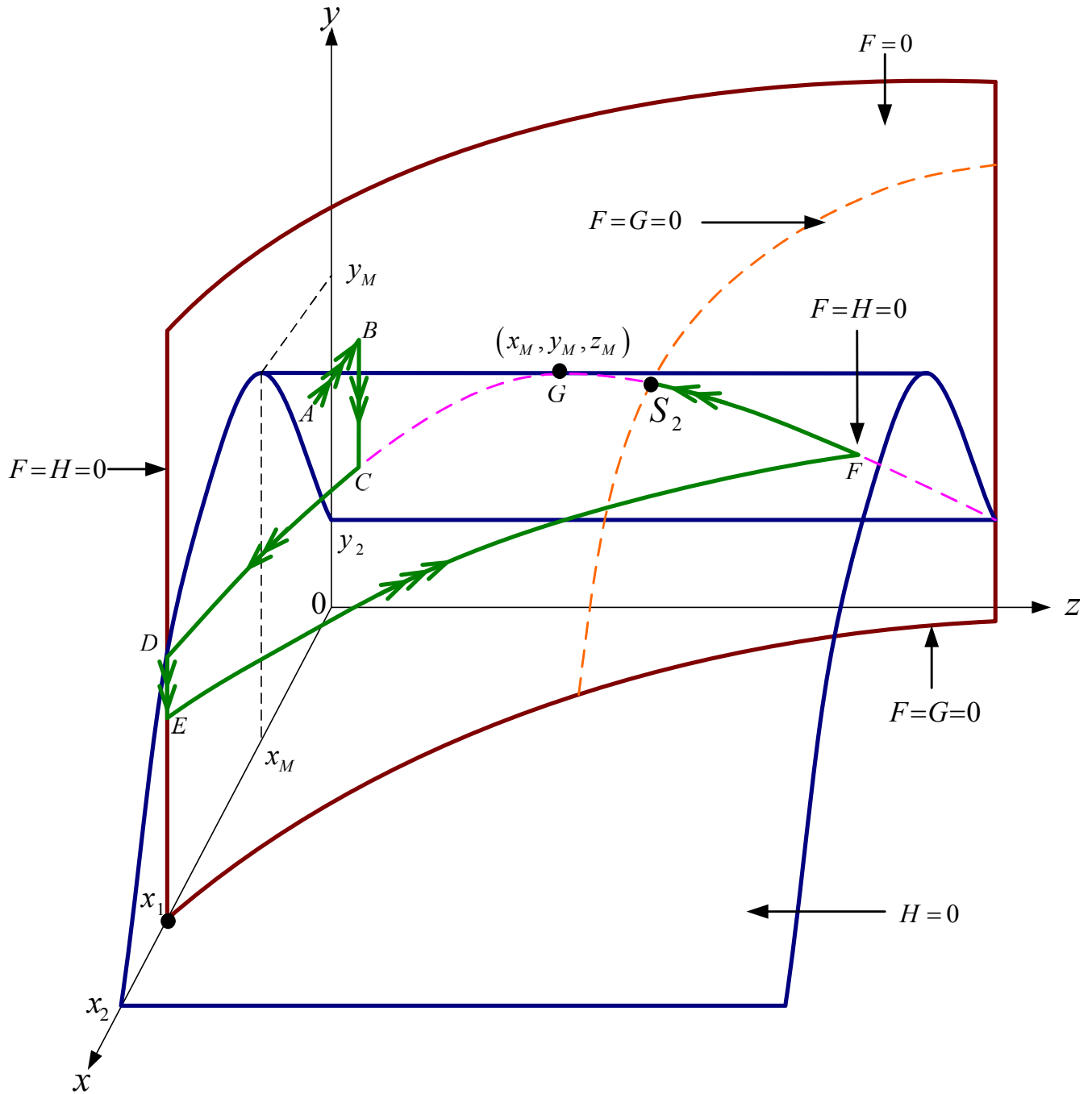


Fig. 2 The three equilibrium manifolds $\{F = 0\}$, $\{G = 0\}$ and $\{H = 0\}$ in (x, y, z) -space in Case 2 . Segments of the trajectories with one, two, and three arrows represent slow, intermediate, and fast transitions, respectively.

Case 3 If ε and δ are sufficiently small, and

$$x_M < x_2 < x_1 \tag{31}$$

$$z_M < z_{S_2} \tag{32}$$

provided that the inequalities (16), (18) and (24)-(26) are satisfied where all parametric values are defined as above, then a stable equilibrium point exists for the system of (4)-(6).

If all inequalities identified in Case 3 hold, then the manifolds $\{F=0\}$, $\{G=0\}$ and $\{H=0\}$ are positioned as in Fig. 3. Starting from point A in front of the manifold $\{F=0\}$. Since $\{F < 0\}$ here, a fast transition will bring the system to the point B on the manifold $\{F=0\}$ in the direction

of decreasing x . Here, $\{G < 0\}$ and a transition at intermediate speed will be made in the direction of decreasing y until point C on the curve $\{F=G=0\}$ is reached. A slow transition then follows along this curve in the direction of increasing z until the steady state S_1 where $\{F=G=H=0\}$ is reached since $\{H > 0\}$ here. Thus, the solution trajectory is expected in this case to tend toward this stable equilibrium point S_1 as time passes.

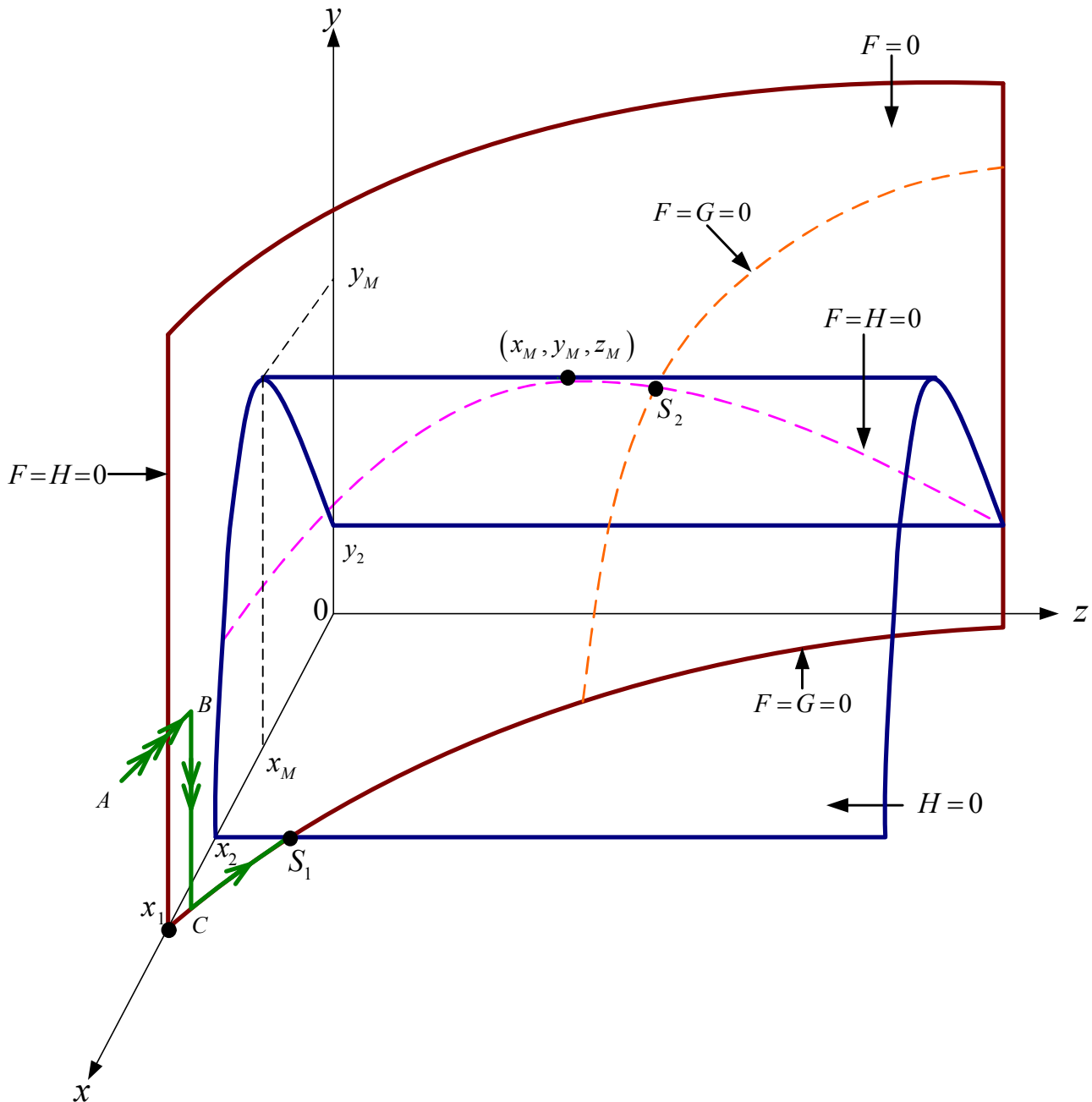


Fig. 3 The three equilibrium manifolds $\{F=0\}, \{G=0\}$ and $\{H=0\}$ in (x, y, z) -space in Case 3. Segments of the trajectories with one, two, and three arrows represent slow, intermediate, and fast transitions, respectively.

IV. NUMERICAL INVESTIGATION

A numerical result of the system (4)-(6) is presented in Fig. 4, with parametric values chosen to satisfy the inequalities identified in Case 1. The solution trajectory,

shown in Fig. 4a project onto the (x, y) -plane, tends to a limit cycle as theoretically predicted. The corresponding time courses of the PTH, CT, and calcium concentration are as shown in Fig. 4b, 4c, and 4d respectively.

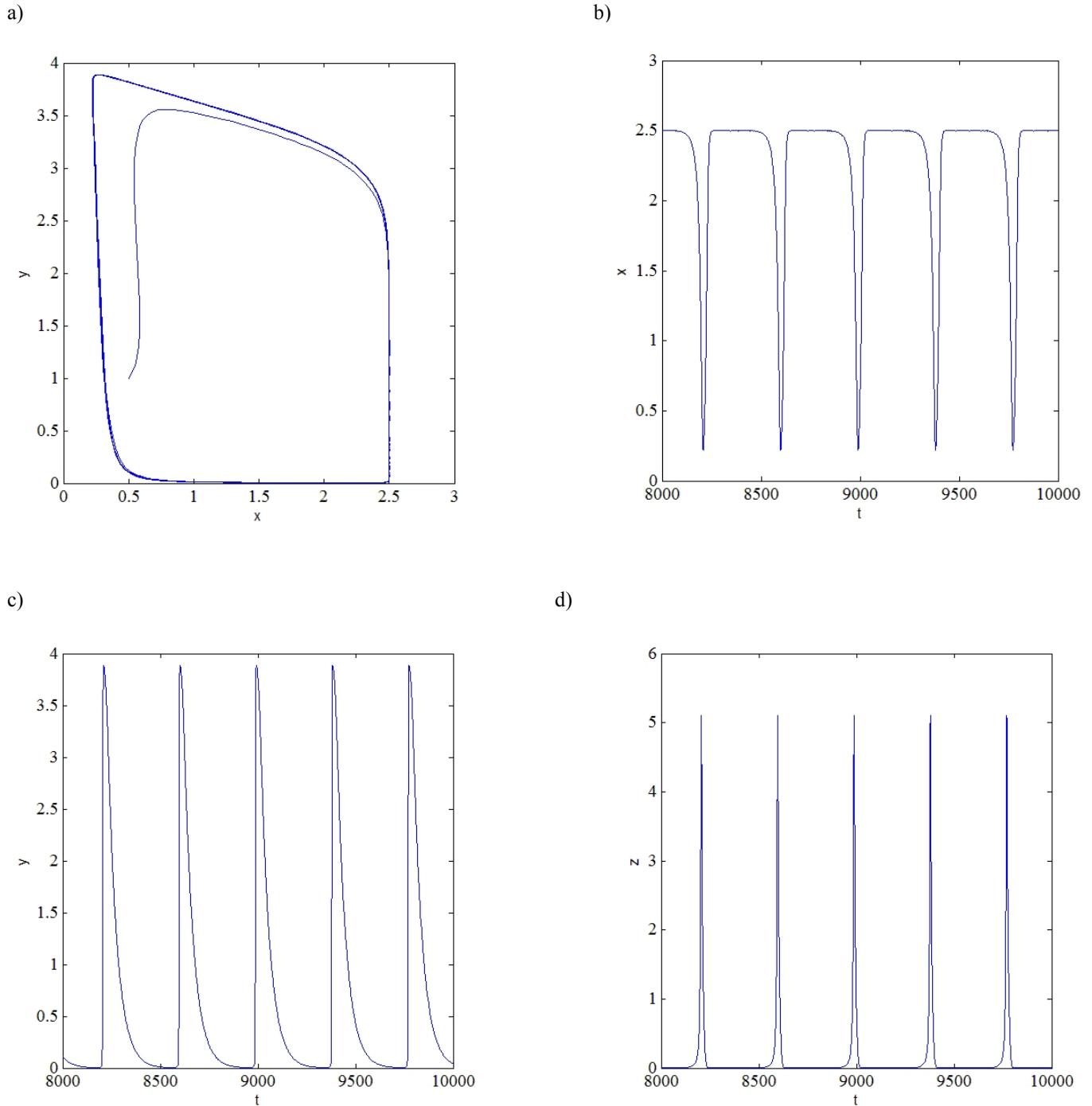


Fig. 4 A computer simulation of the model systems (4)-(6) with $c_1 = 0.5$, $c_2 = 0.4$, $c_3 = 0.1$, $c_4 = 0.4$, $c_5 = 0.9$, $c_6 = 0.3$, $k_1 = 0.4$, $k_2 = 0.6$, $d_1 = 0.5$, $d_2 = 0.03$, $d_3 = 0.25$, $\varepsilon = 0.7$, $\delta = 0.5$, $x(0) = 0.5$, $y(0) = 1$, $z(0) = 1$. (a) The solution trajectory projected onto the (x, y) -plane. (b) The corresponding time courses of PTH concentration (x), (c) CT concentration (y), and (d) calcium concentration (z), respectively.

A numerical result of the system (4)-(6) is presented in Fig. 5, with parametric values chosen to satisfy the inequalities identified in Case 2. The solution trajectory, shown in Fig. 5a project onto the (x,y) -plane, tends to a

stable equilibrium as theoretically predicted. The corresponding time courses of the PTH, CT, and calcium concentration are as shown in Fig. 5b, 5c, and 5d respectively.

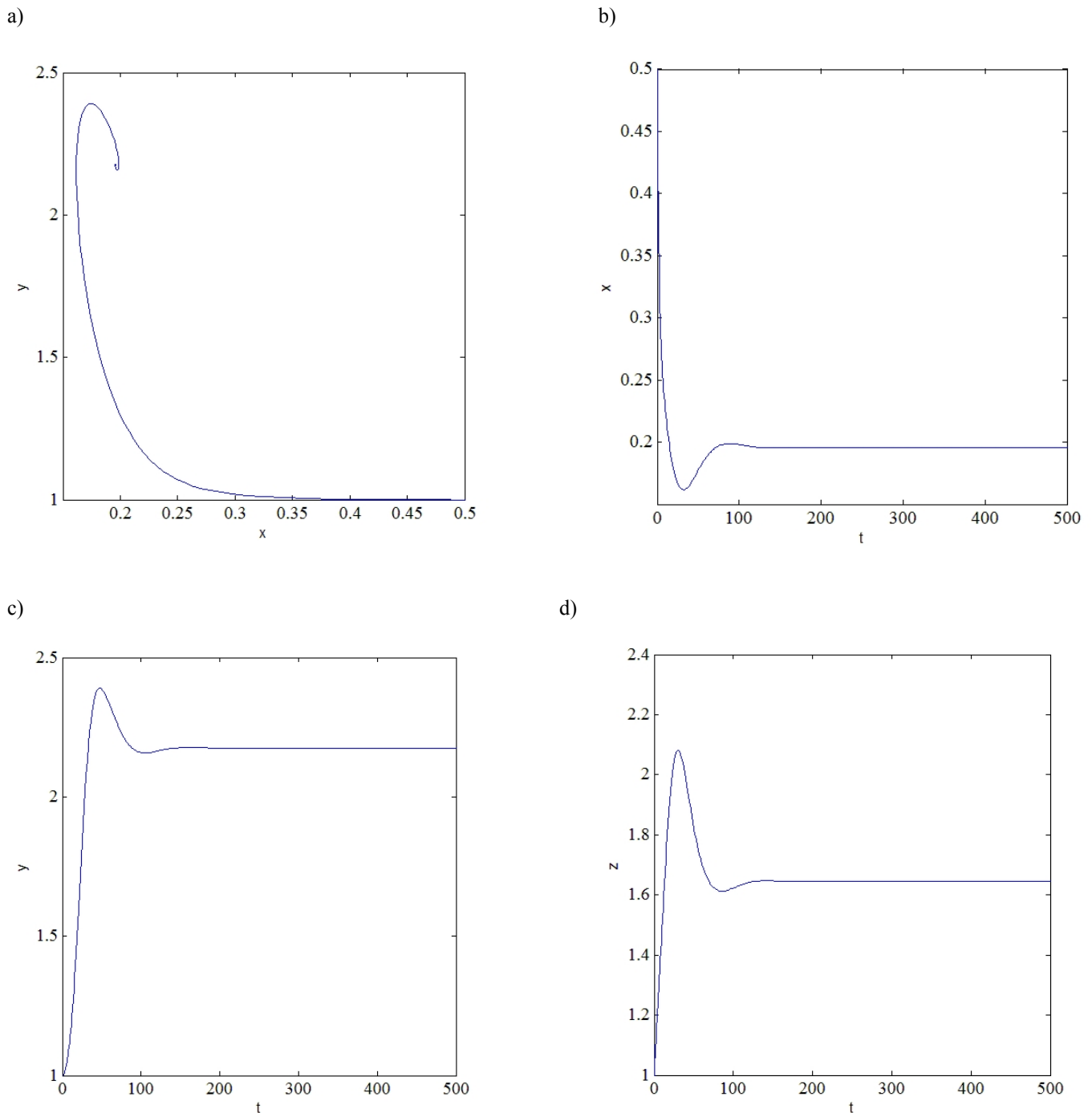


Fig. 5 A computer simulation of the model systems (4)-(6) with $c_1 = 0.2$, $c_2 = 0.4$, $c_3 = 0.1$, $c_4 = 0.4$, $c_5 = 0.9$, $c_6 = 0.3$, $k_1 = 0.4$, $k_2 = 0.6$, $d_1 = 0.5$, $d_2 = 0.3$, $d_3 = 0.25$, $\varepsilon = 0.2$, $\delta = 0.5$, $x(0) = 0.5$, $y(0) = 1$, $z(0) = 1$. (a) The solution trajectory projected onto the (x,y) -plane. (b) The corresponding time courses of PTH concentration (x), (c) CT concentration (y), and (d) calcium concentration (z), respectively.

A numerical result of the system (4)-(6) is presented in Fig. 6, with parametric values chosen to satisfy the inequalities identified in Case 3. The solution trajectory, shown in Fig. 6a project onto the (x,y) -plane, tends to a

stable equilibrium as theoretically predicted. The corresponding time courses of the PTH, CT, and calcium concentration are as shown in Fig. 6b, 6c, and 6d respectively.

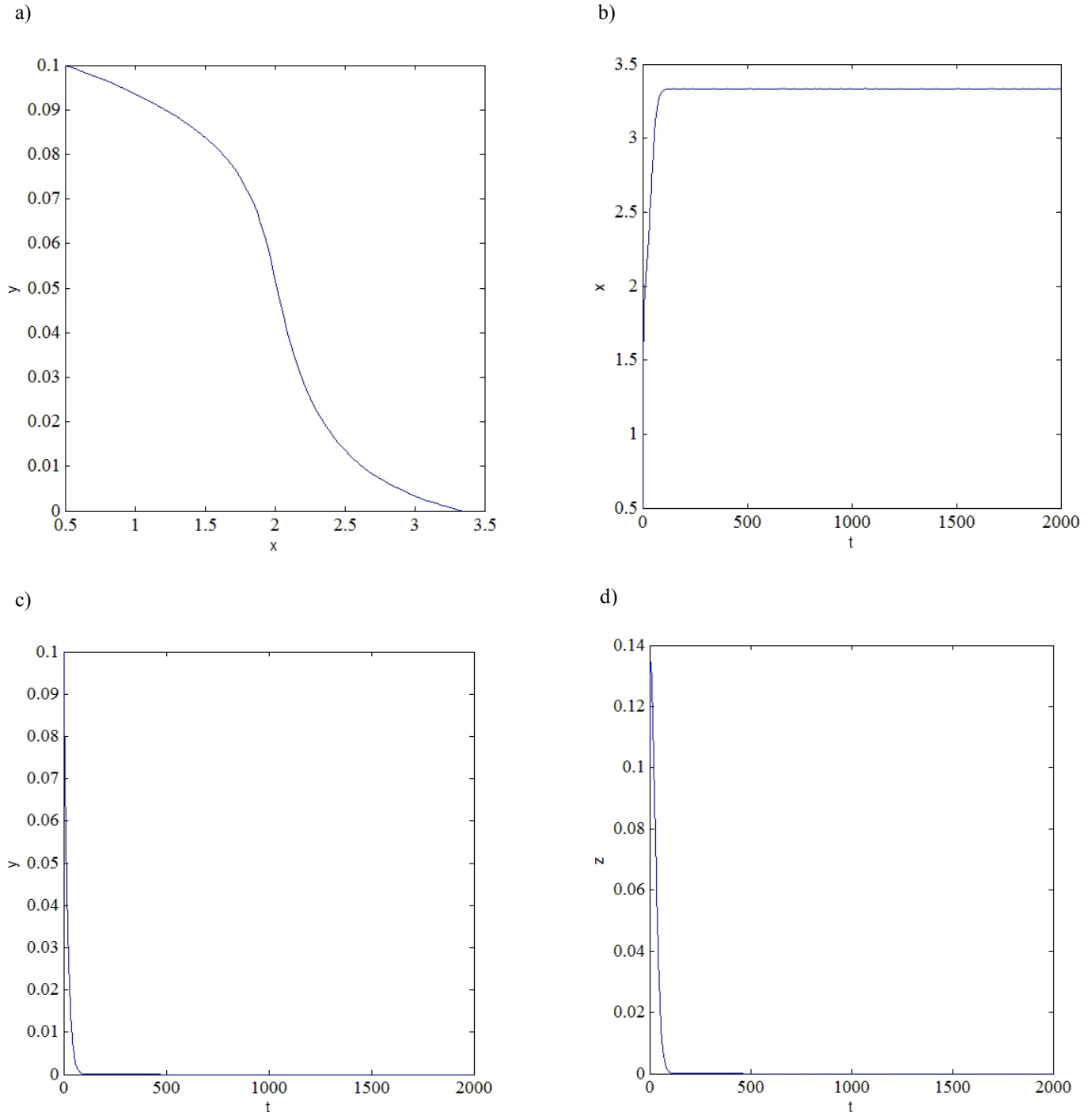


Fig. 6 A computer simulation of the model systems (4)-(6) with $c_1 = 0.2$, $c_2 = 0.3$, $c_3 = 0.1$, $c_4 = 0.4$, $c_5 = 0.9$, $c_6 = 0.3$, $k_1 = 0.2$, $k_2 = 0.7$, $d_1 = 0.3$, $d_2 = 0.1$, $d_3 = 0.5$, $\varepsilon = 0.8$, $\delta = 0.5$, $x(0) = 0.5$, $y(0) = 0.1$, $z(0) = 0.1$. (a) The solution trajectory projected onto the (x,y) -plane. (b) The corresponding time courses of PTH concentration x , (c) CT concentration y , and (d) calcium concentration z , respectively.

V. CONCLUSION

A mathematical model in form of a system of nonlinear ordinary differential equations is developed in order to represent calcium homeostasis based on the effects of parathyroid hormone and calcitonin. Nonlinear dynamic behaviors of the model are investigated theoretically by means of geometric singular perturbation method. We then obtain the conditions on the model parameters that differentiate various kinds of dynamic behavior. If all inequalities identified in Case 1 are satisfied, a periodic solution can be expected. In Case 2 and 3, if all inequalities in each case are satisfied, a stable equilibrium solution can be expected. Moreover, numerical investigations are also carried out by using the Runge-Kutta method that has been widely used to find an approximation of a solution for the system of ordinary differential equations [8]-[11]. The results confirm our theoretical prediction. Therefore, our model can exhibit the nonlinear behavior that has been observed in the clinical evidence [12], especially in Case I. The periodic behavior exhibited by the model corresponds to the pulsatile patterns observed in the serum levels of PTH, CT and calcium.

REFERENCES

- [1] H.M. Goodman, *Basic Medical Endocrinology*, 3rd edition, Academic Press, 2003.
- [2] S.D. Boden, F.S. Kaplan, "Calcium homeostasis", *Orthop. Clin. North Am.*, vol.21, no.1, pp. 31-42, 1990.
- [3] G.R. Mundy, T.A. Guise, "Hormonal control of calcium homeostasis", *Clin. Chem.*, vol.45, no.8 (B), pp. 1347-1352, 1999.
- [4] G. Carmeliet, S.V. Cromphaut, E. Daci, C. Maes, R. Bouillon, "Disorder of calcium homeostasis, *best practice & research clinical endocrinology & metabolism*, vol.17, no.4, pp. 529-546, 2003.
- [5] E.M. Brown, "Extracellular Ca²⁺ sensing, regulation of parathyroid cell function, and role of Ca²⁺ and other ions as extracellular (first) messengers", *Physiol. Rev.*, vol.71, pp. 371-411, 1991.
- [6] T.J. Kaper, "An introduction to geometric methods and dynamical systems theory for singular perturbation problems. Analyzing multiscale phenomena using singular perturbation methods", *Proc. Symposia Appl. Math.*, vol.56, 1999.
- [7] S. Rinaldi, S. Muratori, "A separation condition for the existence of limit cycle in slow-fast systems", *Appl. Math. Modelling*, vol.15, pp. 312-318, 1991.
- [8] W. Sanprasert, U. Chundang and M. Podisuk, "Integration method and Runge-Kutta method", in *Proc. 15th American Conf. on Applied Mathematics*, WSEAS Press, Houston, USA, 2009, pp. 232.
- [9] M. Racila and J.M. Crolet, "Sinupros: Mathematical model of human cortical bone", in *Proc. 10th WSEAS Inter. Conf. on Mathematics and Computers in Biology and Chemistry*, WSEAS Press, Prague, Czech Republic, 2009, pp. 53.
- [10] N. Razali, R. R. Ahmed, M. Darus and A.S. Rambely, "Fifth-order mean Runge-Kutta methods applied to the Lorenz system", in *Proc. 13th WSEAS Inter. Conf. on Applied Mathematics*, WSEAS Press, Puerto De La Cruz, Tenerife, Spain, 2008, pp. 333.
- [11] A. Chirita, R. H. Ene, R.B. Nicolescu and R.I. Carstea, "A numerical simulation of distributed-parameter systems", in *Proc. 9th WSEAS Inter. Conf. on Mathematical Methods and Computational Techniques in Electrical Engineering*, WSEAS Press, Arcachon, 2007, pp. 70.
- [12] K. N. Muse, S. C. Manolagas, L.J. Deftos, N. Alexander, and S.S.C. Yen, "Calcium-regulating hormones across the menstrual cycle", *J. Clin. Endocrinol. Metab.*, vol.62, no.2, pp.1313-1315, 1986.